



The Effect of Synthesis Parameters on the Electrochemical Performance of $\text{Li}_4\text{Ti}_5\text{O}_{12}$

Fatma KILIÇ DOKAN^{1*}  Şaban PATAT^{2,3} 

¹Department of Chemistry and Chemical Processing Technologies, Kayseri University, Kayseri, Turkey

²Department of Chemistry, Erciyes University, Kayseri, Turkey

³Nanotechnology Research Center, ERNAM, Erciyes University, Kayseri, Turkey

Geliş / Received: 24/08/2021, Kabul / Accepted: 18/03/2022

Abstract

The spinel $\text{Li}_4\text{Ti}_5\text{O}_{12}$ is synthesized by a solid-state method. The effect of the synthesis parameters including lithium content, source of Ti and grinding on the electrochemical performance of $\text{Li}_4\text{Ti}_5\text{O}_{12}$ is investigated to optimize the crystalline size, particle size, surface area, morphology and crystallinity of the synthesized materials. The physical properties are determined by X-ray powder diffraction (XRD), scanning electron microscopy (SEM), N_2 adsorption/desorption and conductivity measurements. The electrochemical properties are investigated by conductivity and galvanostatic charge-discharge measurements. Material characterization and electrochemical measurements indicate that the best electrochemical performance can be obtained by using the Li/Ti molar ratio of 4.25/5, ball milling (BM) and anatase TiO_2 (A) as starting material. $\text{Li}_{4.25}\text{Ti}_5\text{O}_{12}$ A-BM, obtained via ball-mill assisted solid-state method and using anatase TiO_2 as the source of Ti, exhibit the most homogeneous morphology, the least crystal and particle sizes, and highest surface area. The best-performing $\text{Li}_{4.25}\text{Ti}_5\text{O}_{12}$ A-BM delivers a satisfactory performance with a excellent charge capacity (141 mAh/g) and small capacity fading (3.6% after 30 charge-discharge cycles) at a 1 C rate (1C=175 mAh.g⁻¹).

Keywords: Lithium-Ion Batteries, $\text{Li}_4\text{Ti}_5\text{O}_{12}$, Anode Material, Ball Mill (BM)

Sentez Parametrelerinin $\text{Li}_4\text{Ti}_5\text{O}_{12}$ 'nin Elektrokimyasal Performansına Etkisi

Öz

Spinel $\text{Li}_4\text{Ti}_5\text{O}_{12}$, katı hal yöntemiyle sentezlenmiştir. Sentezlenen malzemelerin kristal boyutunu, partikül boyutunu, yüzey alanını, morfolojisini ve kristallliğini optimize etmek için lityum içeriği, Ti kaynağı ve öğütme gibi sentez parametrelerinin $\text{Li}_4\text{Ti}_5\text{O}_{12}$ 'nin elektrokimyasal performansı üzerindeki etkisi araştırılmıştır. Fiziksel özellikler, X-ışını toz kırınımı (XRD), taramalı elektron mikroskobu (SEM), N_2 adsorpsiyon/desorpsiyon ve iletkenlik ölçümleri ile belirlenmiştir. Elektrokimyasal özellikler, iletkenlik ve galvanostatik şarj-deşarj ölçümleri ile araştırılmıştır. Malzeme karakterizasyonu ve elektrokimyasal ölçümler, en iyi elektrokimyasal performansın Li/Ti molar oranı 4.25/5, bilyalı öğütme (BM) ve anataz TiO_2 (A) başlangıç malzemesi olarak kullanılarak elde edilebileceğini göstermektedir. Bilyalı değirmen destekli katı hal yöntemiyle ve Ti kaynağı olarak anataz TiO_2 kullanılarak elde edilen $\text{Li}_{4.25}\text{Ti}_5\text{O}_{12}$ A-BM, en homojen morfolojiyi, en iyi kristal ve parçacık boyutlarını ve en yüksek yüzey alanını sergiler. En iyi performans gösteren $\text{Li}_{4.25}\text{Ti}_5\text{O}_{12}$ A-BM, mükemmel şarj kapasitesi (141 mAh/g) ve düşük kapasite kaybı (30 şarj-deşarj döngüsünden sonra %3,6) ile 1 C akımda (1C=175 mAh.g) tatmin edici bir performans sunar.

Anahtar Kelimeler: Lityum-iyon bataryalar, $\text{Li}_4\text{Ti}_5\text{O}_{12}$, Anot materyali, Bilyeli Değirmen

1. Introduction

The development of rechargeable batteries in recent years has increased in parallel with their use in daily life [1]. Extensive research efforts have been mostly focused on cathode/anode materials because they play a decisive role in its electrochemical properties. Recently, much attention has been paid to the research and development of alternative anode candidates to replace the traditional commercially used graphite and other materials.

Lithium titanate, $\text{Li}_4\text{Ti}_5\text{O}_{12}$ (LTO), has attracted significant interest as an alternative anode material for lithium-ion batteries due to its excellent safety characteristics and long lifetime [2-5]. Unlike the carbon anode, $\text{Li}_4\text{Ti}_5\text{O}_{12}$ has a stable operating voltage of ~ 1.5 V vs. Li^+/Li , above the decomposition potential of electrolyte [6]. $\text{Li}_4\text{Ti}_5\text{O}_{12}$ is classified as zero-strain material since there is no structural or volume change during lithium insertion/extraction process. The zero-strain insertion characteristic provides a material with an excellent cycling performance [7]. In comparison to the carbonaceous anode, spinel lithium titanate, $\text{Li}_4\text{Ti}_5\text{O}_{12}$, has better electrochemical performance and higher safety [8]. In addition, the $\text{Li}_4\text{Ti}_5\text{O}_{12}$ anode can accommodate up to three lithium ions per formula unit; this allows a theoretical capacity of 175 mA h g^{-1} in the spinel structure with negligible volume change during charging and discharging [8]. However, the pure $\text{Li}_4\text{Ti}_5\text{O}_{12}$ powder has a low electrical conductivity at room temperature ($< 10^{-13} \text{ S cm}^{-1}$). Since the oxidation state of Ti in $\text{Li}_4\text{Ti}_5\text{O}_{12}$ is the highest possible valence (+4) for Ti, $\text{Li}_4\text{Ti}_5\text{O}_{12}$ is an inferior electronic conductor [9]. Several approaches to overcome this problem have focused on optimizing the synthesis parameters. The design and synthesis of various morphologies and phases are essential subjects in recent studies because they ultimately determine the lithium-ion batteries' performance through influencing electrical, optical, and other properties. Various studies have been reported for the synthesis of lithium titanates, such as conventional solid-state methods [10–12], sol-gel method [13-15], hydrothermal or solvothermal method [16-23], and other synthesis routes have been exploited to prepare $\text{Li}_4\text{Ti}_5\text{O}_{12}$ materials. Among them, conventionally, the solid-state method is used for the synthesis of spinel $\text{Li}_4\text{Ti}_5\text{O}_{12}$ because it is simple and easy.

In this study, spinel $\text{Li}_4\text{Ti}_5\text{O}_{12}$ was synthesized by the solid-state method. The effects of the lithium content, grinding, and precursors on the structure of material and electrochemical performance were analyzed. The results show that the best electrochemical performance can be obtained by using Li/Ti molar ratio of 4.25/5.0, ball milling (BM) and anatase TiO_2 (A) as precursors.

2. Materials and Methods

2.1. Synthesis of $\text{Li}_{4-x}\text{Ti}_5\text{O}_{12}$

During the synthesis of $\text{Li}_4\text{Ti}_5\text{O}_{12}$ at high temperature, a portion of the lithium sublimates and some rutile TiO_2 impurity is obtained as a result of the deterioration of stoichiometry. Due to the sublimation of lithium during high temperature synthesis, the lithium/titanium ratio must be optimized to obtain pure $\text{Li}_4\text{Ti}_5\text{O}_{12}$. $\text{Li}_4\text{Ti}_5\text{O}_{12}$ was synthesized by the solid

state method using a slight excess of Li according to $\text{Li/Ti} = 4/5$ stoichiometry to compensate for high temperature lithium loss in the optimization of the Li/Ti ratio. To synthesize $\text{Li}_{4+x}\text{Ti}_5\text{O}_{12}$ ($x=0.0, 0.05, 0.15, 0.25$) powders, stoichiometric amounts of Li_2CO_3 and anatase (A) TiO_2 were mixed with pestle and mortar and heated in a furnace at 800°C for 12h in air. The $\text{Li}_{4+x}\text{Ti}_5\text{O}_{12}$ with $x=0.25$ among the synthesized materials was found to be pure (see Fig.1). Therefore, the stoichiometry for precursors was hereafter chosen as $\text{Li}_{4.25}\text{Ti}_5\text{O}_{12}$.

In order to find the effect of precursors on the structure and electrochemical performance, $\text{Li}_4\text{Ti}_5\text{O}_{12}$ was synthesized by the solid-state method in a furnace at 800°C for 12h in air using Li_2CO_3 and anatase and rutile TiO_2 as the starting materials. To find the effect of grinding on the structure and electrochemical performance of $\text{Li}_4\text{Ti}_5\text{O}_{12}$, the stoichiometric mixtures of starting materials for $\text{Li}_{4.25}\text{Ti}_5\text{O}_{12}$ were ground with pestle and mortar (PM) or ball-milled (BM) for 12 h using ZrO_2 balls in absolute ethanol, dried in an oven at 100°C , and heated in a furnace at 800°C for 12 h in air. The synthesized powders are named as $\text{Li}_{4.25}\text{Ti}_5\text{O}_{12}\text{R-PM}$, $\text{Li}_{4.25}\text{Ti}_5\text{O}_{12}\text{R-BM}$, $\text{Li}_{4.25}\text{Ti}_5\text{O}_{12}\text{A-PM}$, $\text{Li}_{4.25}\text{Ti}_5\text{O}_{12}\text{A-BM}$ depending on the type of TiO_2 starting material used and grinding method. PM, BM, A and R stand for pestle and mortar, ball-mill, anatase and rutile.

2.2 Materials Characterization

X-ray diffraction (XRD, D8 Advance, Bruker) measurements were carried out to determine the phase compositions, crystallinity and the lattice parameters of the synthesized materials using $\text{CuK}\alpha$ radiation with $\lambda = 0.1545$ nm at 40 kV and 40 mA. The diffraction data were collected in the 2θ range of $10\text{-}90^\circ$ with step size of 0.02° . XRD powder patterns were indexed and unit cell parameters were calculated by using DiffracPlus and Win-Metric programs. The crystal size, t , was calculated from XRD powder pattern according to Sherrer formula:

$$t = \frac{0.94\lambda}{\beta \cos\theta} \quad (1)$$

Where t is the thickness of the crystal (in angstroms), λ the x-ray wavelength, θ the Bragg angle, and β the peak width in radians at half-peak height. The β was calculated from the XRD pattern by using the Topas program.

The surface morphology, particle size and particle size distribution of all samples were investigated using field emission scanning electron microscope (FE-SEM, Zeiss), operated at an accelerating voltage of 20 kV. The samples were laid on carbon tape before being measured and covered with Au-Pd alloy under high vacuum.

The conductivity of all samples was measured by linear scanning voltammetry technique at room temperature. The powder samples were pelleted under a pressure of approximately 9 tons using a 13 mm diameter stainless steel die. The prepared samples were placed in a two-electrode Swagelok type cell and measured with AMETEK Princeton Applied Research VersaSTAT MC model multi-channel galvanostat/potentiostat. The resistance

was calculated from the slope ($\Delta V/\Delta I$) of current versus potential curve given in Eqs. (2)-(4);

$$R=V/I \quad (2)$$

$$\rho = R \frac{S}{l} \quad (3)$$

$$\chi = \frac{1}{\rho} = \frac{l}{SR} \quad (4)$$

where, V is the voltage in mV, I the current in mA, R the resistance in ohm, ρ the resistivity in ohm.cm, S the surface area of the disc in cm^2 , l the thickness of the disc in cm and χ the DC conductivity in S.cm^{-1} ($\text{ohm}^{-1}.\text{cm}^{-1}$).

Surface area measurements of the samples were measured by performing nitrogen gas adsorption/desorption on the Micromeritic Gemini IV. Before measurements, the samples were degassed for 24 hours at 120 °C. The specific surface area of samples was calculated with the Brunauer-Emmett-Teller (BET) method.

2.3 Electrochemical Characterization

For preparation of the electrodes, the active material was mixed with polyvinylidene fluoride (PVDF) as a binder and super P (Conductive Carbon Black) as conductive agent in the weight ratio of 85:10:5 in N-Methyl-2-pyrrolidone (NMP) solvent to get a slurry. The obtained slurry was pasted onto a piece of 13 mm diameter Cu foil wrapped with stainless steel mesh, kept in a vacuum oven overnight at 120°C to remove the solvent (NMP), pressed under two tons of pressure, and finally dried at 120°C for 4h under dynamic vacuum using the Schlenk line, respectively, before taken to an Ar filled glove box. The active material loading to the electrode ranged from 6 to 8 mg cm^{-2} by mass. The cell was assembled in an Ar filled glove-box using the $\text{Li}_4\text{Ti}_5\text{O}_{12}$ electrode as a working electrode, pure lithium metal discs (Merck) with 13 mm diameter both as a counter and a reference electrode, a glass fiber filter as a separator and 1M LiPF_6 (Sigma-Aldrich) in a 1:1 (v/v) solvent mixture of ethylene carbonate and diethyl carbonate (EC/DEC) as the electrolyte. The constant current charge/discharge measurements were carried out in the potential range of 1.0-2.8V at a current density of 1C (175 mA g^{-1}) on an AMETEK Princeton Applied Research VersaSTAT MC model multi-channel galvanostat/potentiostat. All electrochemical measurements were made at room temperature.

Purification of Ethylene Carbonate [39]: Ethylene carbonate (EC) was dried overnight on phosphorus pentoxide (P_2O_5), then subjected to fractional distillation under dynamic vacuum and taken to the argon chamber without contact with air. The distillate was incubated overnight on a previously dried Linda 5A molecular sieve to minimize trace water.

Purification of Diethyl Carbonate [39]: 100 mL of diethyl carbonate (DEC) was washed with 20 mL of 10% Na_2CO_3 , 20 mL of saturated CaCl_2 and finally 30 mL of water. Then 5g of anhydrous CaCl_2 was stirred and filtered for two hours, then the same amount of anhydrous CaCl_2 was stirred and filtered for one hour. Finally, fractional distillation was

carried to the argon cabinet without contact with air. To minimize the water content, it was placed on a previously dried Linda 5A type molecular sieve.

Purification of Acetylene Black [39]: To remove the oil in acetylene black (carbon black), 1:1 by weight of concentrated HCl was added to it and stirred for 24 hours. The mixture was filtered and washed several times with distilled water to remove the remaining HCl. After air-drying at room temperature, it was stirred with benzene and acetone for one day. The material dried again at room temperature was heated in a vacuum oven at $600\text{ }^\circ\text{C}$ for 24 hours to remove adsorbed gases.

3. Results and Discussion

XRD powder patterns of the synthesized $\text{Li}_{4+x}\text{Ti}_5\text{O}_{12}$ ($x = 0, 0.05, 0.15, 0.25$) materials are given in Fig.1. As shown in Fig. 1, All samples show very high crystallinity, which is especially important for charge-discharge measurements at high temperatures [40]. All the diffraction peaks of $\text{Li}_{4.25}\text{Ti}_5\text{O}_{12}$ can be indexed to the cubic spinel structure of $\text{Li}_4\text{Ti}_5\text{O}_{12}$ with space group $\text{Fd}3\text{m}$ (JCPDS no 49-0207) [41]. Besides the $\text{Li}_4\text{Ti}_5\text{O}_{12}$ diffraction peaks, there are the impurity peaks of TiO_2 (rutile) at $2\theta=27.45$ and 54.35 in XRD patterns of $\text{Li}_{4+x}\text{Ti}_5\text{O}_{12}$ ($x = 0, 0.05, 0.15$). These indicate that the pure spinel $\text{Li}_4\text{Ti}_5\text{O}_{12}$ can be successfully synthesized at the Li:Ti molar ratio of 4.25:5.0 by the solid-state method.

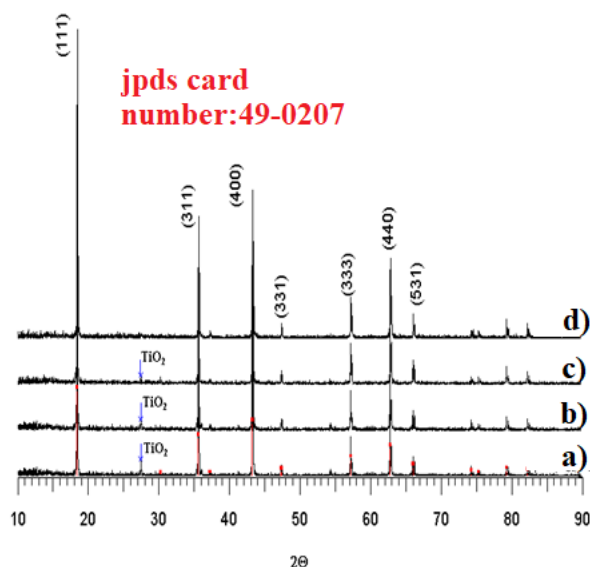


Fig.1. XRD patterns of $\text{Li}_{4+x}\text{Ti}_5\text{O}_{12}$ a) $x = 0$, b) 0.05 , c) 0.15 , d) 0.25

The XRD diffraction patterns of $\text{Li}_{4.25}\text{Ti}_5\text{O}_{12}\text{R-PM}$, $\text{Li}_{4.25}\text{Ti}_5\text{O}_{12}\text{R-BM}$, $\text{Li}_{4.25}\text{Ti}_5\text{O}_{12}\text{A-PM}$, and $\text{Li}_{4.25}\text{Ti}_5\text{O}_{12}\text{A-BM}$ samples are given in Fig.2. All the XRD patterns matched well with the diffraction patterns of the $\text{Li}_4\text{Ti}_5\text{O}_{12}$ cubic phase with the space group Fd-3m (JCPDS:49-0207), revealing the high purity of the as prepared samples.

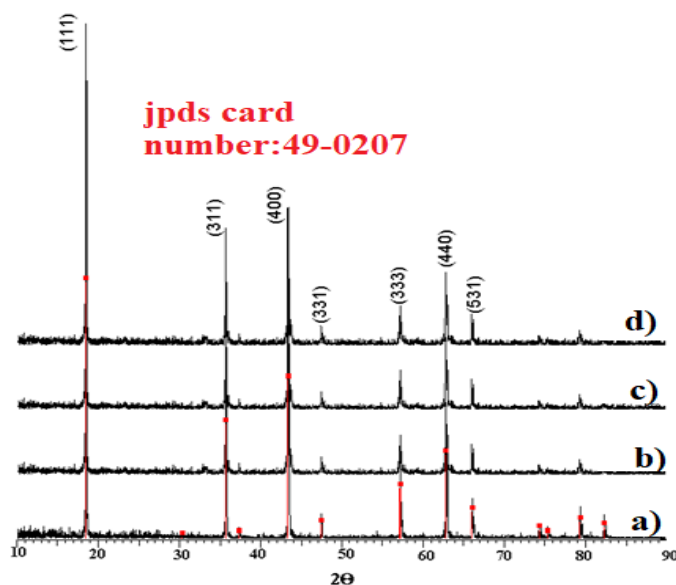


Fig.2. XRD patterns of a) $\text{Li}_{4.25}\text{Ti}_5\text{O}_{12}\text{R-PM}$, b) $\text{Li}_{4.25}\text{Ti}_5\text{O}_{12}\text{R-PM}$, c) $\text{Li}_{4.25}\text{Ti}_5\text{O}_{12}\text{A-BM}$ and d) $\text{Li}_{4.25}\text{Ti}_5\text{O}_{12}\text{R-BM}$ samples

Crystal size calculated using the (111) diffraction peak, and unit cell parameter of the samples are given in Table 1. The unit cell parameter (8.336\AA) and crystallite size (122 nm) of the $\text{Li}_{4.25}\text{Ti}_5\text{O}_{12}\text{A-BM}$ among the samples are the smallest, indicating that grinding the precursor of $\text{Li}_{4.25}\text{Ti}_5\text{O}_{12}$ with a ball-mill and using anatase TiO_2 as a starting materials reduce the crystal size and unit cell parameter.

Table 1. Average crystallite size, unit cell parameter, particle size, conductivity and surface area of $\text{Li}_{4.25}\text{Ti}_5\text{O}_{12}\text{R-PM}$, $\text{Li}_{4.25}\text{Ti}_5\text{O}_{12}\text{R-BM}$, $\text{Li}_{4.25}\text{Ti}_5\text{O}_{12}\text{A-PM}$ and $\text{Li}_{4.25}\text{Ti}_5\text{O}_{12}\text{A-BM}$ samples

Sample	Average crystallite size (nm)	Unit cell parameter (\AA)	Particle size (nm)	Conductivity (S cm^{-1})	at
$\text{Li}_{4.25}\text{Ti}_5\text{O}_{12}\text{R-PM}$	195	8.351	320-360	3.31×10^{-8}	
$\text{Li}_{4.25}\text{Ti}_5\text{O}_{12}\text{R-BM}$	156	8.349	270-300	3.84×10^{-8}	
$\text{Li}_{4.25}\text{Ti}_5\text{O}_{12}\text{A-PM}$	145	8.342	220-240	4.22×10^{-8}	
$\text{Li}_{4.25}\text{Ti}_5\text{O}_{12}\text{A-BM}$	122	8.336	200-250	4.72×10^{-8}	

SEM image of the $\text{Li}_{4.25}\text{Ti}_5\text{O}_{12}$ samples and the particle size obtained from it are illustrated in Fig. 3 and Table 1, respectively. It can be seen from Fig. 3 and Table 1 that all the $\text{Li}_4\text{Ti}_5\text{O}_{12}$ samples have regular morphologies and there are no the aggregations of $\text{Li}_{4.25}\text{Ti}_5\text{O}_{12}$ particles with size distribution in the range of approximately 200-360 nm. The particle size of the $\text{Li}_{4.25}\text{Ti}_5\text{O}_{12}\text{A-BM}$ among the samples is the smallest, similar to a trend in crystallite size change obtained from XRD patterns. These results reveal that the use of

ball-mill for grinding the precursors and anatase TiO_2 as a starting material can reduce the particle size and prevent the aggregation of $\text{Li}_{4.25}\text{Ti}_5\text{O}_{12}$ particles. The small particles promise large surface area and a smaller diffusion path for Li^+ and improve the electrochemical performance of the samples.

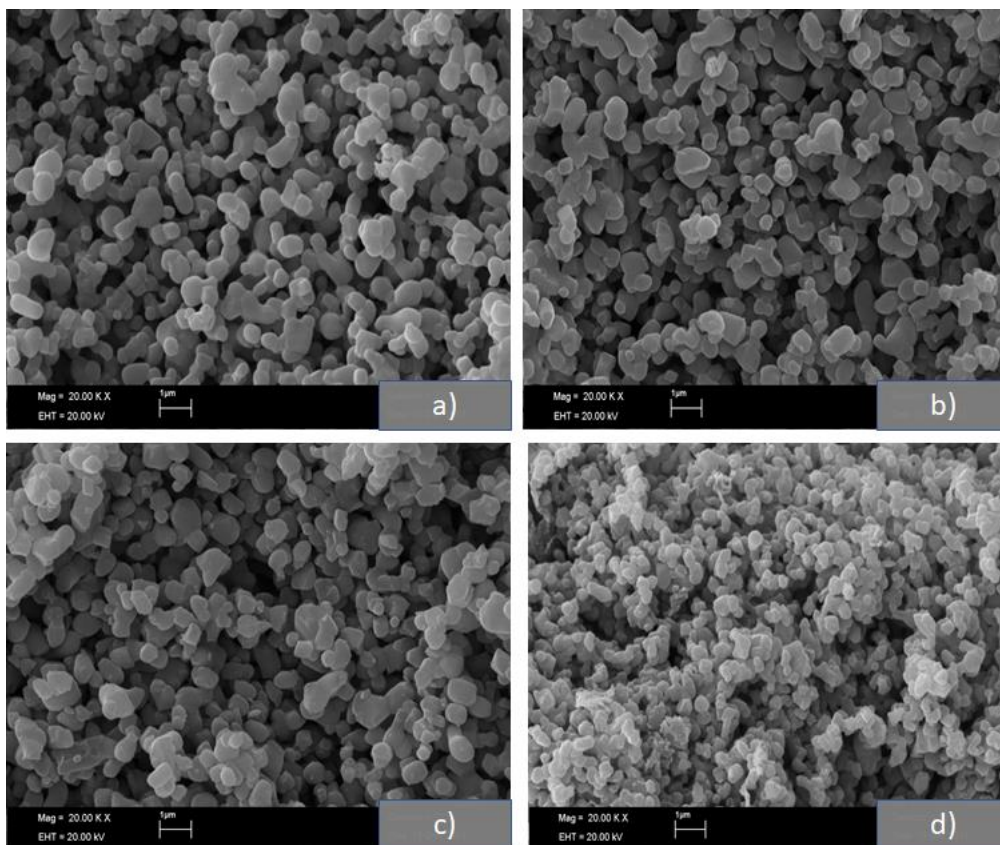


Fig.3. SEM images of a) $\text{Li}_{4.25}\text{Ti}_5\text{O}_{12}\text{R-PM}$, b) $\text{Li}_{4.25}\text{Ti}_5\text{O}_{12}\text{A-PM}$, c) $\text{Li}_{4.25}\text{Ti}_5\text{O}_{12}\text{R-BM}$ and d) $\text{Li}_{4.25}\text{Ti}_5\text{O}_{12}\text{A-BM}$

The electrical conductivity values of $\text{Li}_{4.25}\text{Ti}_5\text{O}_{12}$ are given in Table 1. It can be seen from Table 1 that the $\text{Li}_{4.25}\text{Ti}_5\text{O}_{12}\text{A-BM}$ has the highest conductivity compared to other samples, which is consistent with the change in their crystallite and particle sizes. The particle and crystallite sizes decrease, the electron and Li^+ ion diffusion path becomes shorter, and conductivity increases.

Nitrogen adsorption-desorption isotherms of $\text{Li}_{4.25}\text{Ti}_5\text{O}_{12}$ samples are given in Fig.4. As shown in

Fig.4, all the samples presented a type-IV isotherm with a H3 hysteresis loop, suggesting the presence of rich mesoporous. BET (Brunauer-Emmett-Teller) surface area calculated from adsorption-desorption curves are given in Table 1. According to BET results in Table 1, the $\text{Li}_{4.25}\text{Ti}_5\text{O}_{12}\text{A-BM}$ has the highest specific surface area compared to other samples, which is compatible with their crystallite sizes, particle sizes and conductivities. The higher the surface area, the better electrochemical performance of battery will give as the surface area will provide higher conductivity due to higher contact area.

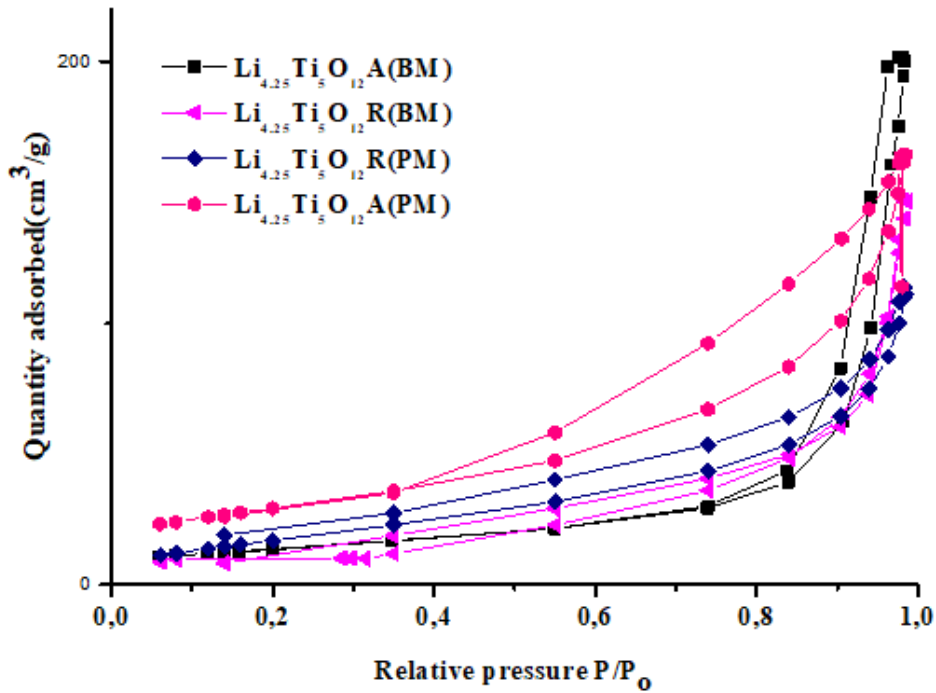


Fig.4. Nitrogen adsorption-desorption isotherms of $\text{Li}_{4.25}\text{Ti}_5\text{O}_{12}$ samples

The charge and discharge curves of the 1st, 10th, 20th and 30th cycles of the $\text{Li}_{4.25}\text{Ti}_5\text{O}_{12}$ samples at 1C ($1\text{C}=175\text{ mAh g}^{-1}$) in the voltage range of 1-2.8 V vs Li/Li^+ are illustrated in Fig. 4. As shown in Fig. 4, there is a big difference in specific capacity between the first cycle and the next cycles, which can be attributed to the irreversible changes of the inside of the batteries such as lithium being trapped in the materials and the decomposition of electrolyte. All the samples demonstrate the charge and discharge plateaus at around ~1.60-1.80 and ~1.40-1.55 V respectively, corresponding to the reversible phase transition between $\text{Li}_4\text{Ti}_5\text{O}_{12}$ and $\text{Li}_7\text{Ti}_5\text{O}_{12}$ during Li^+ -ion insertion/extraction process. The $\text{Li}_{4.25}\text{Ti}_5\text{O}_{12}\text{A-BM}$ electrode has the smallest voltage difference between the charge and discharge plateaus, ΔE ($E_{\text{charge}}-E_{\text{discharge}}$), which is related to the polarization degree, compared to the $\text{Li}_{4.25}\text{Ti}_5\text{O}_{12}\text{R-PM}$, $\text{Li}_{4.25}\text{Ti}_5\text{O}_{12}\text{R-BM}$ and $\text{Li}_{4.25}\text{Ti}_5\text{O}_{12}\text{A-PM}$ electrodes. The low polarization degree of the $\text{Li}_{4.25}\text{Ti}_5\text{O}_{12}\text{A-BM}$ electrode can be related to its high conductivity, small crystallite size and particle size.

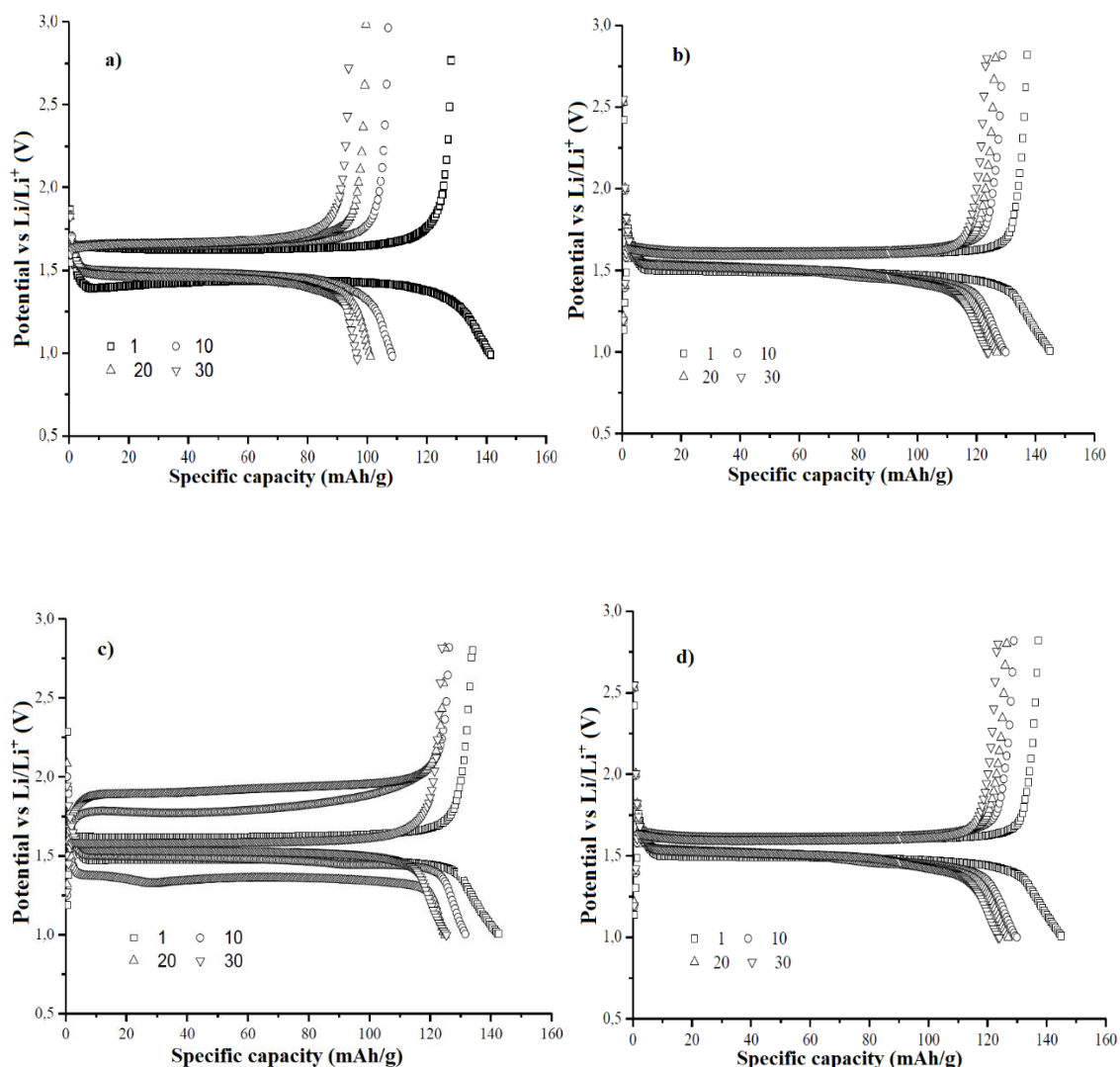


Fig. 5. Galvanostatic charge/discharge curves of the 1st, 10th, 20th and 30th cycles of the $\text{Li}_{4.25}\text{Ti}_5\text{O}_{12}$ electrodes at 1C (1C=175 mAh g^{-1}) current density in the voltage range of 1-2.8 V vs Li/Li⁺ **a)** $\text{Li}_{4.25}\text{Ti}_5\text{O}_{12}\text{R-PM}$, **b)** $\text{Li}_{4.25}\text{Ti}_5\text{O}_{12}\text{R-BM}$, **c)** $\text{Li}_{4.25}\text{Ti}_5\text{O}_{12}\text{A-PM}$ and **d)** $\text{Li}_{4.25}\text{Ti}_5\text{O}_{12}\text{A-BM}$

The cycle performance at 1C current density in the voltage range of 1.0-2.8 V vs Li/Li⁺ and coulombic efficiency of the $\text{Li}_{4.25}\text{Ti}_5\text{O}_{12}$ electrodes are illustrated in Fig. 5a and 5b, respectively. From Fig. 5a, the 1st (2nd) discharge capacities of $\text{Li}_{4.25}\text{Ti}_5\text{O}_{12}\text{R-PM}$, $\text{Li}_{4.25}\text{Ti}_5\text{O}_{12}\text{R-BM}$, $\text{Li}_{4.25}\text{Ti}_5\text{O}_{12}\text{A-PM}$ and $\text{Li}_{4.25}\text{Ti}_5\text{O}_{12}\text{A-BM}$ electrodes were 141.4(129.6), 145.0(136.2), 142.0(134) and 141.1(133.4) mAh g^{-1} , respectively. And the discharge capacity retention of $\text{Li}_{4.25}\text{Ti}_5\text{O}_{12}\text{R-PM}$, $\text{Li}_{4.25}\text{Ti}_5\text{O}_{12}\text{R-BM}$, $\text{Li}_{4.25}\text{Ti}_5\text{O}_{12}\text{A-PM}$ and $\text{Li}_{4.25}\text{Ti}_5\text{O}_{12}\text{A-BM}$ electrodes after 30 charge/discharge cycles at 1C were 74.6%, 91.1%, 93.5% and 96.4% of the second discharge capacity, respectively. The high capacity retention of the $\text{Li}_{4.25}\text{Ti}_5\text{O}_{12}\text{A-BM}$ electrode can be attributed to its high conductivity, small crystallite size and particle size [42-43]. According to Fig. 5b, Coulombic efficiency of the 1st (3rd) cycle of the $\text{Li}_{4.25}\text{Ti}_5\text{O}_{12}\text{R-PM}$, $\text{Li}_{4.25}\text{Ti}_5\text{O}_{12}\text{R-BM}$, $\text{Li}_{4.25}\text{Ti}_5\text{O}_{12}\text{A-PM}$ and $\text{Li}_{4.25}\text{Ti}_5\text{O}_{12}\text{A-BM}$ electrodes were 91.0(98.4) %, 94.5(97.7) %, 95.2(96.9) % and 97.2(99.5)%, respectively, which indicates good reversibility for the removal and insertion

of Li-ion in $\text{Li}_{4.25}\text{Ti}_5\text{O}_{12}$ electrodes. The higher initial discharge capacity is associated with the irreversible capacity and the slightly reduced coulombic yields can be attributed to side reactions with the electrolyte and the formation of a solid electrolyte film. (SEI) [44].

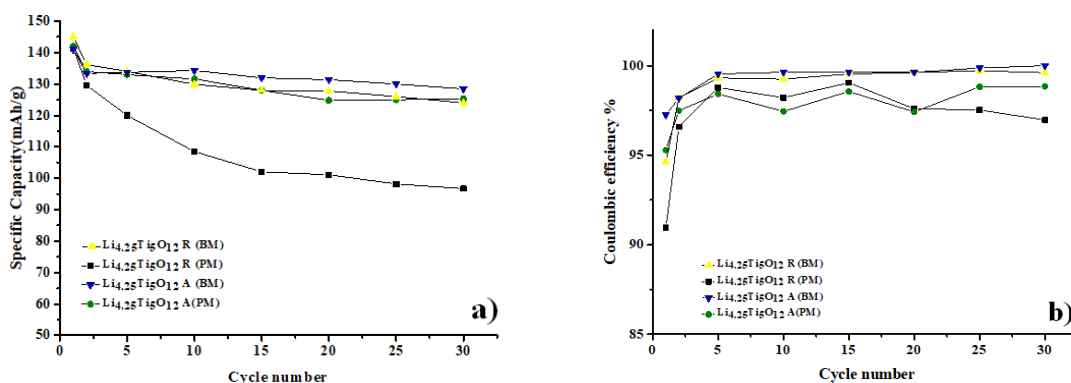


Fig. 6. a) cycle performance, and b) Coulombic efficiency of the $\text{Li}_{4.25}\text{Ti}_5\text{O}_{12}$ electrodes at 1C current density in the voltage range of 1.0-2.8 V vs Li/Li^+

The rate capabilities of the $\text{Li}_{4.25}\text{Ti}_5\text{O}_{12}\text{R-PM}$, $\text{Li}_{4.25}\text{Ti}_5\text{O}_{12}\text{R-BM}$, $\text{Li}_{4.25}\text{Ti}_5\text{O}_{12}\text{A-PM}$ and $\text{Li}_{4.25}\text{Ti}_5\text{O}_{12}\text{A-BM}$ electrodes at various current rates in the potential range of 1.0 and 2.8 V are shown in Fig. 6. In general, the discharge specific capacities of all four electrodes decrease as the current density increased. The rate capability of the $\text{Li}_{4.25}\text{Ti}_5\text{O}_{12}\text{R-PM}$ at all current rates is worse than those of the $\text{Li}_{4.25}\text{Ti}_5\text{O}_{12}\text{R-BM}$, $\text{Li}_{4.25}\text{Ti}_5\text{O}_{12}\text{A-PM}$ and $\text{Li}_{4.25}\text{Ti}_5\text{O}_{12}\text{A-BM}$ electrodes, which can be due to its low conductivity and big particle sizes. The high-rate capabilities of the $\text{Li}_{4.25}\text{Ti}_5\text{O}_{12}\text{A-BM}$ electrode at 5.0C and 10.0C can be attributed to its high conductivity.

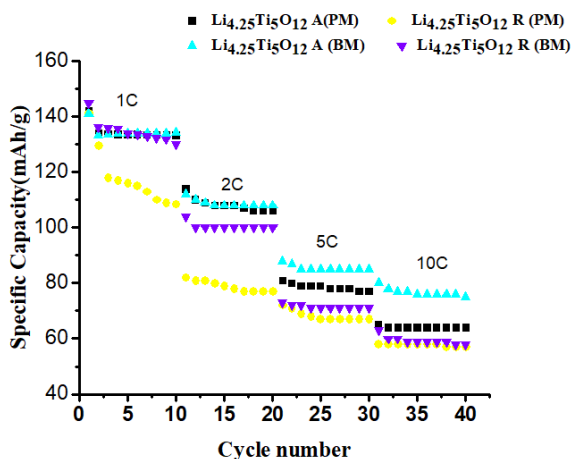


Fig.6. Rate capabilities of the the $\text{Li}_{4.25}\text{Ti}_5\text{O}_{12}$ electrodes at 1C, 2C,5C and 10C currents in the potential range of 1.0 and 2.8 V vs Li/Li^+ .

In summary, the electrochemical performance of the $\text{Li}_4\text{Ti}_5\text{O}_{12}\text{A-BM}$ anode material, synthesized by using anatase TiO_2 and Li_2CO_3 as starting materials with a Li:Ti molar ratio of 4.25/5.0 and grinding the precursor with ball-mill, is comparable with the literature data given Table 2.

Table 2. Comparison of the electrochemical performance of $\text{Li}_4\text{Ti}_5\text{O}_{12}$ anode materials synthesized by the solid-state method.

Starting material, grinding process and heat treatment medium	1 st (30 th) cycle discharge capacity values at 1C current density (mAh/g)	1 st (30 th) cycle discharge capacity values at different current density (mAh/g)	Particle size (nm)	Potential range studied
a)anatase TiO_2 , Li_2CO_3 , ball mill b)anatase TiO_2 , high energy ball mill, heating in air [43]	a)102.4 b)165.3	a)90 at 2C and 80 at 4C b)145 at 2C and 125 at 4C	a)271 b)204	1.0-2.8 V
a)anatase TiO_2 , Li_2CO_3 , agate and mortar b)anatase TiO_2 , Li_2CO_3 , high energy ball mill, heating in air [44]	a)127.9 (120.2) b)151.7(149.7)	-----	a) 1070 b) 480	1.0-2.5 V
Anatase TiO_2 , Li_2CO_3 , high energy ball mill, heating in air [45]	160	164.7 at 0.5C and 70.6(66.7) at 10C	300-800	1.0-3V
Anatase TiO_2 , Li_2CO_3 , high energy ball mill, heating in air [46]	155	168 at 0.1C and 89 at 10C	242	1.0-2.6 V
LiCl , TiCl_4 , oxalic acid, heating in air [47]	133(131.6)	167(166) at 0.5C	Porous Particles	1.0-2.5 V
LiOH , nano TiO_2 , ultrasonic dispensing heating in air [48]	154	125 at 5C and 115 at 10C	<100	1.0-2.5 V
Anatase, Li_2CO_3 , ball-mill, heating in air This work	141.1(128.6)	85 at 5.0C and 75 at 10.0C	200-250	1.0-2.8

4. Conclusions

The pure $\text{Li}_4\text{Ti}_5\text{O}_{12}$ anode material for lithium ion batteries has been successfully synthesized by solid-state method using anatase TiO_2 and Li_2CO_3 as starting materials with a Li: Ti molar ratio of 4.25/5.0. The effect of Ti sources and grinding the precursor on electrochemical performance of the $\text{Li}_4\text{Ti}_5\text{O}_{12}$ anode electrode is investigated. The $\text{Li}_4\text{Ti}_5\text{O}_{12}$ A-BM anode, synthesized by using anatase TiO_2 and Li_2CO_3 as starting materials with a Li: Ti molar ratio of 4.25/5.0 and grinding the precursor with ball-mill, demonstrates the highest 1st cycle Coulombic efficiency of 97.2% and the capacity retention of ~96.4% after after 30 charge/discharge cycles at 1.0C current density. The high Coulombic efficiency and the high capacity retention of the $\text{Li}_4\text{Ti}_5\text{O}_{12}$ A-BM electrode can be attributed to its small crystal and particle sizes and high surface area, leading to both high electronic

and ionic conductivity. All these results highlights the potential use of $\text{Li}_4\text{Ti}_5\text{O}_{12}$ -BM as anode material for lithium ion batteries.

Ethics in Publishing

There are no ethical issues regarding the publication of this study.

Author Contributions

Designing the study, collecting data; Evaluation of the results and writing of the article were done by Fatma KILIÇ DOKAN and Şaban PATAT.

Acknowledgments

This work has been supported financially by Scientific Research Projects Unit of Erciyes University (with the Project Number FBD-10-3314), which is gratefully acknowledged by the authors. We would also like to thank Altınay Boyraz, an employee of the Erciyes University Technology Research and Application Center, for interest in performing the analyses in this study.

References

- [1] Z. Yang, D. Choi, S. Kerisit, K.M. Rosso, D. Wang, J. Zhang, G. Graff, J. Liu., (2009) Nanostructures and lithium electrochemical reactivity of lithium titanites and titanium oxides: A review, *J Power Sources*, 192588-598.
- [2] T. Ohzuku, A. Ueda and N. Yamamoto., (1995) Zero-Strain Insertion Material of $\text{Li}[\text{Li}_{1/3}\text{Ti}_{5/3}] \text{O}_4$ for Rechargeable Lithium Cells *J. Electrochem. Soc.*, 142, 1431.
- [3] K. Zaghib, M. Simoneau, M. Armand and M. Gauthier., (1999) Electrochemical study of $\text{Li}_4\text{Ti}_5\text{O}_{12}$ as negative electrode for Li-ion polymer rechargeable batteries, *J. Power Sources*, 81, 300.
- [4] K. Nakahara, R. Nakajima, T. Matsushima and H. Majima., (2003) Preparation of particulate $\text{Li}_4\text{Ti}_5\text{O}_{12}$ having excellent characteristics as an electrode active material for power storage cells, *J. Power Sources*, 117, 131.
- [5] T.F. Yi, L.J. Jiang, J. Shu, C.B. Yue, R.S. Zhu and H.B. Qiao., (2010) Recent development and application of $\text{Li}_4\text{Ti}_5\text{O}_{12}$ as anode material of lithium ion battery, *J. Phys. Chem. Solids*, 71, 1236.

- [6] K. Mukai, Y. Kato and H. Nakano., (2014) Understanding the Zero-Strain Lithium Insertion Scheme of $\text{Li}[\text{Li}_{1/3}\text{Ti}_{5/3}]\text{O}_4$: Structural Changes at Atomic Scale Clarified by Raman Spectroscopy *J. Phys. Chem. C*, 118, 6, 2992–2999.
- [7] S. Huang, Z. Wen, X. Zhu, Z. Lin., (2007) Effects of dopant on the electrochemical performance of $\text{Li}_4\text{Ti}_5\text{O}_{12}$ as electrode material for lithium ion batteries, *Journal of Power Sources*, 165, 408.
- [8] J. Gao, C. Jiang, J. Ying, C. Wan., (2006) Preparation and characterization of high-density spherical $\text{Li}_4\text{Ti}_5\text{O}_{12}$ anode material for lithium secondary batteries *Journal of Power Sources*, 155, 364.
- [9] C.H. Chen, J.T. Vaughey, A.N. Jansen, D.W. Dees, A.J. Kahaiovn, T. Goacher, M.M. Thackeray., (2001) Studies of Mg-Substituted $\text{Li}_{4-x}\text{Mg}_x\text{Ti}_5\text{O}_{12}$ Spinel Electrodes ($0 \leq x \leq 1$) for Lithium Batteries, *J. Electrochem. Soc.* 148 A102–A104.
- [10] Huang, S., Wen, Z., Zhu, X., Lin, Z., (2007) Effects of dopant on the electrochemical performance of $\text{Li}_4\text{Ti}_5\text{O}_{12}$ as electrode material for lithium ion batteries. *J. Power Sources* 165, 408–412.
- [11] Chen, C.H., Vaughey, J.T., Jansen, A.N., Dees, D.W., Kahaian, A.J., Goacher, T., Thackeray, M.M., (2001) Studies of Mg-substituted $\text{Li}_{4-x}\text{Mg}_x\text{Ti}_5\text{O}_{12}$ spinel electrodes (0 B x B 1) for lithium batteries. *J. Electrochem. Soc.* 148, A102–A104.
- [12] Wolfenstine, J., Allen, J.L., (2008) Electrical conductivity and chargecompensation in Ta doped $\text{Li}_4\text{Ti}_5\text{O}_{12}$. *J. Power Sources* 180,582–585.
- [13] Jiang, C., Ichihara, M., Honma, I., Zhou, H., (2007) Effect of particledispersion on high rate performance of nano-sized $\text{Li}_4\text{Ti}_5\text{O}_{12}$ anode. *Electrochim. Acta* 52, 6470–6475.
- [14] Sorensen, E.M., Barry, S.J., Jung, H.-K., Rondinelli, J.R., Vaughey, J.T., Poeppelmeier, K.R., (2006) Three-dimensionally ordered macroporous $\text{Li}_4\text{Ti}_5\text{O}_{12}$: effect of wall structure on electrochemical properties. *Chem. Mater.* 18, 482–489.
- [15] Bach, S., Pereira-Ramos, J.P., Baffier, N., (1999) Electrochemical properties of sol-gel $\text{Li}_{4/3}\text{Ti}_{5/3}\text{O}_4$. *J. Power Sources* 81–82, 273–276.
- [16] Y. Li, H. Zhao, Z. Tian, W. Qiu, X. Li., (2008) Solvothermal synthesis and electrochemical characterization of amorphous lithium titanate materials, *J. Alloys Compd.*, 455, 471.
- [17] J. Chen, L. Yang, S. Fang, Y. Tang., (2010) Synthesis of sawtooth-like $\text{Li}_4\text{Ti}_5\text{O}_{12}$ nanosheets as anode materials for Li-ion batteries, *Electrochimica Acta*, 55, 6596.

- [18] Y. Tang, L. Yang, S. Fang, Z. Qiu., (2009) $\text{Li}_4\text{Ti}_5\text{O}_{12}$ hollow microspheres assembled by nanosheets as an anode material for high-rate lithium ion batteries, *Electrochimica Acta*, 54, 6244.
- [19] D. K. Lee, H. W. Shim, J. S. An, C. M. Cho, I. S. Cho, K. S. Hong, D. W. Kim., (2010) Synthesis of Heterogeneous $\text{Li}_4\text{Ti}_5\text{O}_{12}$ Nanostructured Anodes with Long-Term Cycle Stability, *Nanoscale Research Letters*, 5, 1585.
- [20] S. C. Lee, S. M. Lee, J. W. Lee, J. B. Lee, S. S. Han, H. C. Lee, H. J. Kim., (2009) Spinel $\text{Li}_4\text{Ti}_5\text{O}_{12}$ Nanotubes for Energy Storage Materials, *Journal of Physical Chemistry C*, 113, 18420.
- [21] L. Shen, C. Yuan, H. Luo, X. Zhang, K. Xu, Y. Xia, Facile synthesis of hierarchically porous $\text{Li}_4\text{Ti}_5\text{O}_{12}$ microspheres for high rate lithium ion batteries†, *Journal of Materials Chemistry* 2010, 20, 6998.
- [22] Y. F. Tang, L. Yang, Z. Qiu, J. S. Huang.,(2008), Preparation and electrochemical lithium storage of flower-like spinel $\text{Li}_4\text{Ti}_5\text{O}_{12}$ consisting of nanosheets,*Electrochemistry Communications*, 10, 1513.
- [23] J. Li, Z. Tang, Z. Zhang., (2005) Controllable formation and electrochemical properties of one-dimensional nanostructured spinel $\text{Li}_4\text{Ti}_5\text{O}_{12}$, *Electrochemistry Communications*, 7, 894.
- [24] Guerfi, A., Se´vigny, S., Lagace´, M., Hovington, P., Kinoshita, K., Zaghbi, K., (2003) Nano-particle $\text{Li}_4\text{Ti}_5\text{O}_{12}$ spinel as electrode for electrochemical generators. *J. Power Sources* 119–121, 88–94.
- [25] Baohua Li, Feng Ning, Yan-Bing He, Hongda Du , Quan-Hong Yang , Jun Ma , Feiyu Kang ,Chin-Tsau Hsu., (2011) Synthesis and Characterization of Long Life $\text{Li}_4\text{Ti}_5\text{O}_{12}/\text{C}$ Composite Using Amorphous TiO_2 Nanoparticles *Int. J. Electrochem. Sci.*, 63210 – 3223.
- [26] Lu, H., Wang,J., Stoller, M., Wang, T., Bao, Y. ve Hao H. 2016. "An Overview of Nanomaterials for Water and Wastewater Treatment." *Advances in Materials Science and Engineering* 2016: 10.
- [27] Ahmed H. Hammad, MSh Abdel-wahab, Sajith Vattamkandathil, Akhalakur Rahman Ansari., (2018) Structural and optical properties of ZnO thin films prepared by RF sputtering at different thicknesses. *Physica B* 540, 1–8.
- [28] Cheng L, Yan J, Zhu GN, Luo JY, Wang CX, Xia YY (2010) General synthesis of carbon-coated nanostructure $\text{Li}_4\text{Ti}_5\text{O}_{12}$ as a high rate electrode material for Li-ion intercalation. *J Mater Chem* 20(3):595–602.

- [29] Chang-Hoon Hong, Ji Heon Ryu, Jaemyung Kim, Dang-Hyok Yoon., (2012) Effects of the starting materials and mechanochemical activation on the properties of solid-state reacted $\text{Li}_4\text{Ti}_5\text{O}_{12}$ for lithium ion batteries, *Ceramics International* 38 301–310.
- [30] S.W. Han et al., (2013) Solid-state synthesis of $\text{Li}_4\text{Ti}_5\text{O}_{12}$ for high power lithium ion battery applications *Journal of Alloys and Compounds* 570 144–149.
- [31] Prising PP, Mancini R, Petrucci L, Contini V, Villano P., (2001) $\text{Li}_4\text{Ti}_5\text{O}_{12}$ as anode in all-solid-state, plastic, lithium-ion batteries for low-power applications, *Solid State Ionics*;144:185–92.
- [32] Li J, Jin YL, Zhang XG, Yang H., (2007) Microwave solid-state synthesis of spinel $\text{Li}_4\text{Ti}_5\text{O}_{12}$ nanocrystallites as anode material for lithium-ion batteries, *Solid State Ionics*;178:1590–4.
- [33] Vikram Babu B, Tewodros Aregai G, Vijaya Babu K, Samatha K, Veeraiiah V., (2017) Effect of Calcination Temperature on the Structural Properties of Spinel $\text{Li}_4\text{Ti}_5\text{O}_{12}$ Anode Material for Lithium-Ion Batteries, *Chem Sci Trans*;6(2):1336.
- [34] Zou, J., Gao, J., Xie, F., (2010) An Amorphous TiO_2 Sol Sensitized with H_2O_2 with the Enhancement of Photocatalytic Activity, *Journal of Alloys and Compounds*, 497: pp. 420– 427. <http://dx.doi.org/10.1016/j.jallcom.2010.03.09329>.
- [35] Sean Kelly, Fred H. Pollak, and Micha Tomkiewicz., (1997) Raman Spectroscopy as a Morphological Probe for TiO_2 Aerogels”, *J. Phys. Chem. B*, 101, 14, 2730–2734.
- [36] Colthup, N., Daly, L., (1990) Wiberley, S. *Introduction to Infrared and Raman Spectroscopy* Academic Press: Boston, MA, USA, 29.
- [37] Choi, H.C., Young, M., Seung, B., (2005) Size effects in the Raman spectra of TiO_2 nanoparticles, *Vib. Spect*, 37, 33–38.
- [38] Physical Adsorption Characterization of Nanoporous Materials., (2010) *Characterization of nanoporous materials* 1059 *Chemie Ingenieur Technik Chemie Ingenieur Technik*, 82, 7.
- [39] Zhang, J. J. and Xia, Y. Y., (2006) Co-Sn Alloys as Negative Electrode Materials for Rechargeable Lithium Batteries, *J. Electrochem. Soc*, 153, A1466-1471.
- [40] J. Liu, Y. Shen, L. Chen, Y. Wang, Y. Xia., (2015) Carbon coated $\text{Li}_4\text{Ti}_5\text{O}_{12}$ nanowire with high electrochemical performance under elevated temperature, *Electrochim. Acta*, 156, 38-44.
- [41] L. Wang, H. Zhang, Q. Deng, Z. Huang, A. Zhou, J. Li., (2014) Superior rate performance of $\text{Li}_4\text{Ti}_5\text{O}_{12}/\text{TiO}_2/\text{C}/\text{CNTs}$ composites via microemulsion-assisted method as anodes for lithium ion battery, *Electrochim. Acta*, 142, 202–207.

- [42] Chang-Hoon Hong, Alfian Noviyanto, Ji Heon Ryu, Dang-Hyok Yoon, Jaemyung Kim., (2012) Effects of the starting materials and mechanochemical activation on the properties of solid-state reacted $\text{Li}_4\text{Ti}_5\text{O}_{12}$ for lithium ion batteries *Ceramics international*,38,301-310.
- [43] Wei Liu, Qian Wang, Jian Zhang, Xiaohua Xie, Haohan Liu, Guoquan Min, Baojia Xia., (2016) Isothermal kinetic analysis of the effects of high-energy ball milling on solid-state reaction of $\text{Li}_4\text{Ti}_5\text{O}_{12}$, *Powder Technology*, 287, 373 –379.
- [44] K.T. Kim, C.-Y. Yu, C.S. Yoon, S.-J. Kim, Y.-K. Sun, S.-T. Myung., (2015) Carbon-coated $\text{Li}_4\text{Ti}_5\text{O}_{12}$ nanowires showing high rate capability as an anode material for rechargeable sodium batteries, *Nano Energy*, 2 ,725-734.
- [45] Dan Wang, Xiaoyan Wu, Yaoyao Zhang, Jin Wang, Peng Yan, Chunming Zhang, Dannong He., (2014) The influence of the TiO_2 particle size on the properties of $\text{Li}_4\text{Ti}_5\text{O}_{12}$ anode material for lithium-ion battery *Ceramics international* ,40,3799-3804.
- [46] Seung-Woo Han, Ji Heon Ryu, Joayoung Jeong, Dang-Hyok Yoon., (2013) Solid-state synthesis of $\text{Li}_4\text{Ti}_5\text{O}_{12}$ for high power lithium ion battery applications *Journal of Alloys and Compounds*, 570 144–149.
- [47] Chih-Yuan Lin, Jenq-Gong Duh., (2011) Porous $\text{Li}_4\text{Ti}_5\text{O}_{12}$ anode material synthesized by one-step solid state method for electrochemical properties enhancement, *Journal of Alloys and Compounds* 509 3682–3685.
- [48] Yun-Ho Jin, Kyung-Mi Min, Hyun- Woo Shim, Seung-Deok Seo, In-Sung Hwang, Kyung-Soo Park and Dong-Wan Kim., (2012) Facile synthesis of nano- $\text{Li}_4\text{Ti}_5\text{O}_{12}$ for high-rate Li-ion battery anodes, **Nanoscale Research Letters*, 7:10 <http://www.nanoscalereslett.com/content/7/1/10>.